

Site-selective adsorption of naphthalene-tetracarboxylic-dianhydride on Ag(110): First-principles calculations

Audrius Alkauskas,* Alexis Baratoff, and C. Bruder

Institute of Physics and National Center of Competence in Research “Nanoscale Science”, University of Basel, Klingelbergstrasse 82, CH-4056 Basel, Switzerland

(Dated: October 1, 2018)

The mechanism of adsorption of the 1,4,5,8-naphthalene-tetracarboxylic-dianhydride (NTCDA) molecule on the Ag(110) surface is elucidated on the basis of extensive density functional theory calculations. This molecule, together with its perylene counterpart, PTCDA, are archetype organic semiconductors investigated experimentally over the past 20 years. We find that the bonding of the molecule to the substrate is highly site-selective, being determined by electron transfer to the LUMO of the molecule and local electrostatic attraction between negatively charged carboxyl oxygens and positively charged silver atoms in $[1\bar{1}0]$ atomic rows. The adsorption energy in the most stable site is 0.9eV. A similar mechanism is expected to govern the adsorption of PTCDA on Ag(110) as well.

PACS numbers: 68.43.-h, 73.20.Hb, 71.15Mb

I. INTRODUCTION

The adsorption of functional organic molecules on metal surfaces is of wide current interest both from technological and fundamental points of view. Precise control of the first monolayer is a prerequisite for fabricating high-quality organic thin films, which are the basic constituents of hybrid organic-inorganic optical and electronic devices¹. Understanding molecule-molecule and molecule-substrate interactions is necessary to explain different surface architectures^{2,3}, and knowledge of the local electronic structure⁴ and of mechanical properties is crucial for designing and controlling functionalities at the nanometer scale, for example in the fields of molecular electronics^{5,6} and molecular machines⁷.

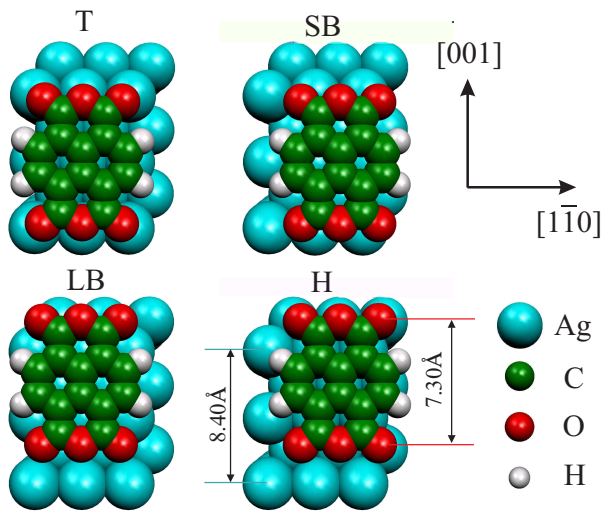


FIG. 1: (Color online) Local adsorption geometries studied: T (top), SB (short bridge), LB (long bridge) and H (hollow). The names refer to the position of the midpoint of the central C=C bond with respect to the underlying Ag(110) surface.

Among the many molecules whose interaction with solid substrates has been studied, NTCDA and its perylene counterpart, PTCDA, deserve special attention due to their unique properties. The aromatic cores of both molecules are terminated at opposite ends by two anhydride groups, as seen in Fig. 1 for NTCDA, and both of them have a D_{2h} symmetry. Upon room temperature deposition on silver surfaces they form commensurate superstructures, which depend on the orientation of the substrate^{3,8,9}. Earlier NEXAFS studies^{10,11,12} of the adsorbed monolayers indicated that both molecules are parallel to the substrate and exhibit substrate-dependent spectral changes which were interpreted as evidence for covalent π -bonding³. The finding that such rather large molecules, which cover \sim 10-15 substrate atoms, can lock into preferred adsorption sites, had no simple explanation for a long time. Chemisorption via π -states delocalized over the aromatic core, claimed to favor the high surface mobility required for self-assembly⁹, cannot easily account for site-selectivity. Recently, Eremtchenko *et al.*^{13,14} proposed an interesting experimental argument that PTCDA binds to Ag(111) via its central aromatic ring, but that this potential reaction center is inactive in the case of unsubstituted perylene. Later Hauschild *et al.*¹⁵ reported synchrotron-quality normal incidence X-ray standing wave (NIXSW) measurements and density functional calculations on the same system, which revealed that anhydride side groups are slightly closer to the substrate than the aromatic core and also contribute to the bonding. Comparison of vibration spectra of adsorbed monolayers of PTCDA on different silver substrates by Tautz *et al.*^{16,17,18} showed, however, that beside common features there are also notable differences in local adsorption properties on different surfaces. The Ag(110) surface consists of a regular array of atomic rows and grooves in the $[1\bar{1}0]$ direction, and one expects (a) the lateral variation of the adsorption energy to be larger for the (110) surface than for (001) and (111) surfaces and (b) charge transfer to be more pronounced (see below). Similar differences should also exist for the adsorption of

NTCDA on silver substrates even though only the electronic structure of the NTCDA/Ag(111) interface has so far been studied in detail^{10,19}.

Our work is directly motivated by the experiments of Fink *et al.*⁸ who investigated the lateral ordering of NTCDA monolayers on several noble metal surfaces by means of LEED, STM and temperature-programmed desorption spectroscopy. Whereas two lateral superstructures were found for NTCDA on Ag(111) and Ag(001), only one simpler superstructure was observed for Ag(110) and Cu(001). The NTCDA/Ag(110) interface, having a well-defined geometry and a relatively small number of atoms per unit cell, is therefore appealing for computational work.

Density functional theory (DFT) calculations²⁰ have proven quite successful in describing covalent and ionic bonding of small molecules at surfaces²¹. However, it is not obvious whether bonding of large closed-shell organic adsorbates on noble metals, where van-der-Waals interactions can play a significant role, will be adequately grasped by current semilocal implementations of DFT, like LDA and GGA²². In general, since dispersion interactions are not taken into account when constructing the current density functionals^{23,24}, one cannot expect a good performance of DFT for pure van-der-Waals-bonded systems. It is unclear, however, how much van-der-Waals character do the molecule-metal bonds possess in the systems that concern us here. Even though the first DFT study of a large organic molecule interacting with a metal appeared almost ten years ago²⁵, still few such works exist. In the case of molecules like C₆₀, which bond strongly to some noble metal substrates²⁶, or when a single head group is involved in the bonding, as for alkane-thiols on Au(111)²⁷, or when reactive metals such as Ni²⁸ are used as substrates, present-day DFT is largely successful. However, a recent study²⁹ showed that calculated DFT adsorption energies of inert hydrocarbons are much smaller than experimental ones. For PTCDA, sometimes no bonding is found, even though experiments suggest a weak chemisorption^{30,31}. On the more open and reactive Ag(110) surface the molecule-metal bond may exhibit a more covalent (or ionic) character for which current density functionals perform rather well. Fortunately, we *do* find that in our case DFT is successful, because much of the relevant experimental data, some extrapolated from related systems, is reproduced by calculations.

II. COMPUTATIONAL DETAILS

Calculations were performed with the ABINIT code³², using the PBE-GGA exchange-correlation functional³³. Light atoms were described with Goedecker-Teter-Hutter pseudopotentials³⁴, and silver atoms were treated within the Troullier-Martins scheme³⁵ (s-component taken as local to avoid ghost states). The simulated system consisted of a NTCDA molecule on one side of a six-layer silver slab and a vacuum region equivalent to eight sil-

ver layers. Thus the total computational box included 78 atoms and a pool of 690 electrons, making it already a quite demanding system. Wave functions were expanded in plane waves with a 50Ry kinetic energy cutoff (60 and 70Ry for test calculations - the results changed little) The Brillouin zone of the 3×3 surface unit cell was sampled by six special k-points³⁶ together with a Fermi broadening of 0.01Ha.

The bottom three silver layers were fixed in their calculated bulk positions (PBE lattice constant 4.20 Å), and the top three silver layers and the molecular degrees of freedom were relaxed according to Hellmann-Feynman forces, preserving the initial local symmetry. Geometry optimization was performed using damped molecular dynamics until the maximum force was below 10⁻³ Ha/bohr. The potential energy surface describing the metal-molecule interaction is rather shallow, meaning that a substantial change in geometry leads only to a minor change in total energy. This motivated our strict convergence criterion. As test calculations, we calculated surface energies of clean silver surfaces, and obtained 0.32, 0.41 and 0.62 eV per surface atom for (111), (001) and (110) faces in accord with previous GGA results and the experimental trend. The calculated work functions for these surfaces were 4.47, 4.27 and 4.13 eV, respectively, typical values for PBE using Troullier-Martins pseudopotentials. These values are also in accord with the experimental trend: the closed-packed (111) surface has the highest work function (4.46-4.74eV) while the open (110) has the lowest work function among the low-index silver surfaces (4.14-4.52eV). This is quite important for the present system: the Ag(110) surface, having a smaller work function, can donate more charge to electron acceptor molecules like NTCDA. These differences in work functions are certainly relevant for an interpretation of adsorption properties of the molecules of interest on different substrates^{16,17,18}.

III. RESULTS AND DISCUSSION

After minimizing the residual forces, we obtained the following adsorption energies: 0.92eV for the T site, 0.45eV for SB, and practically zero for LB and H. The adsorption energies were determined using the relationship $E_{ad} = -(E_{tot} - E_{sub} - E_{mol})$, where E_{sub} is the total energy of the bare slab (calculated using the same computational box), E_{mol} is the total energy of an isolated NTCDA molecule (calculated using a large enough computational box), and E_{tot} is the total energy of substrate-adsorbate system. Positive adsorption energy means exothermic adsorption. The experimental adsorption energy for NTCDA on Ag(110) is not known. For a superstructure of NTCDA on Ag(001) with a similar area per molecule (100.2 Å² vs 106.4 Å²) a value of about 1.0eV was obtained from the temperature-programmed desorption spectrum⁸, while for a denser superstructure of NTCDA on Ag(111) an adsorption energy of 1.1eV was

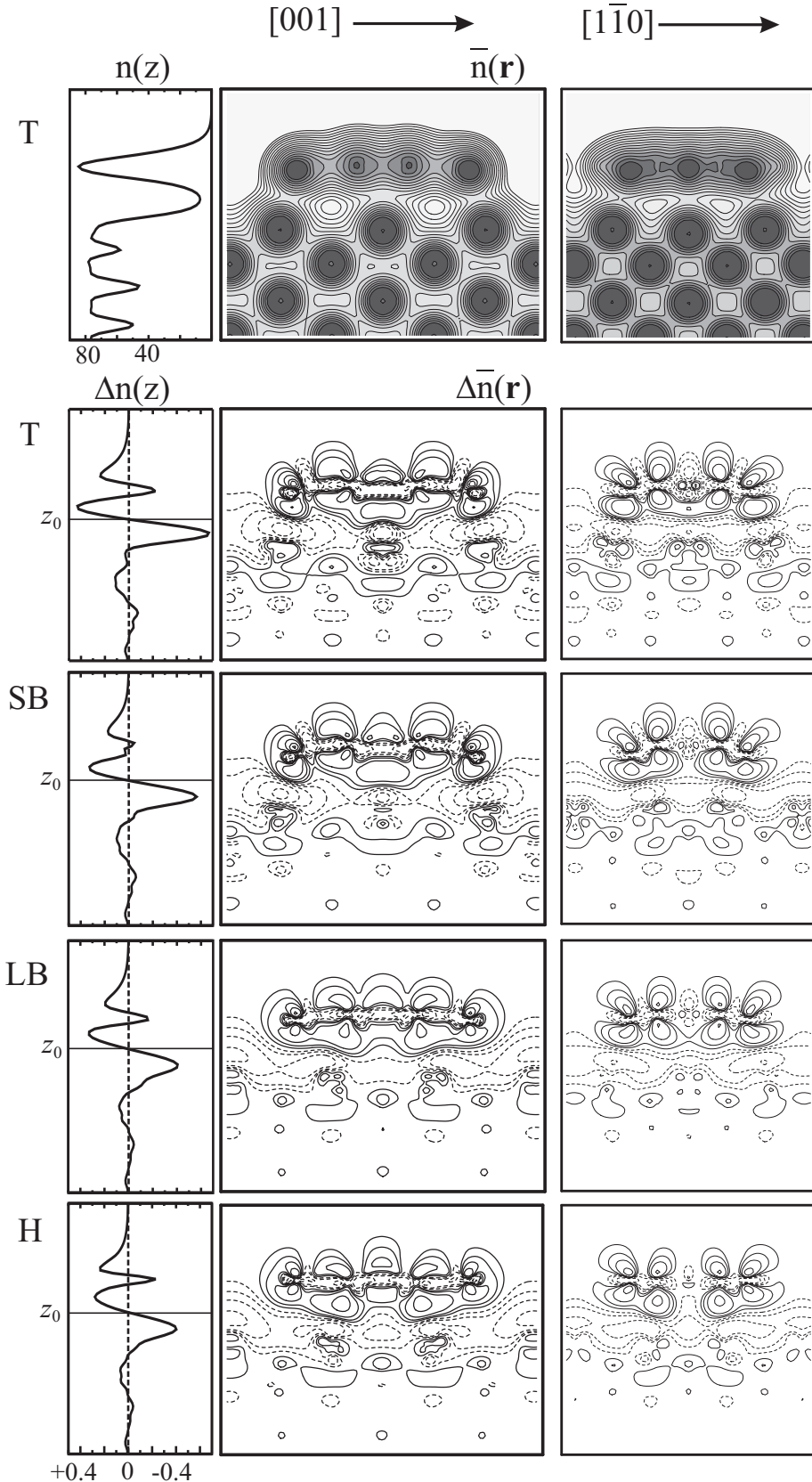


FIG. 2: Total electron density for the top site (upper row) and density differences for all four adsorption sites. Left column: xy -integrated densities (the units are $e\text{\AA}^{-1}$). Central column: averages over the $[1\bar{1}0]$ direction. Right: averages over the $[001]$ direction. Solid lines represent electron charge accumulation regions, broken lines - depletion regions.

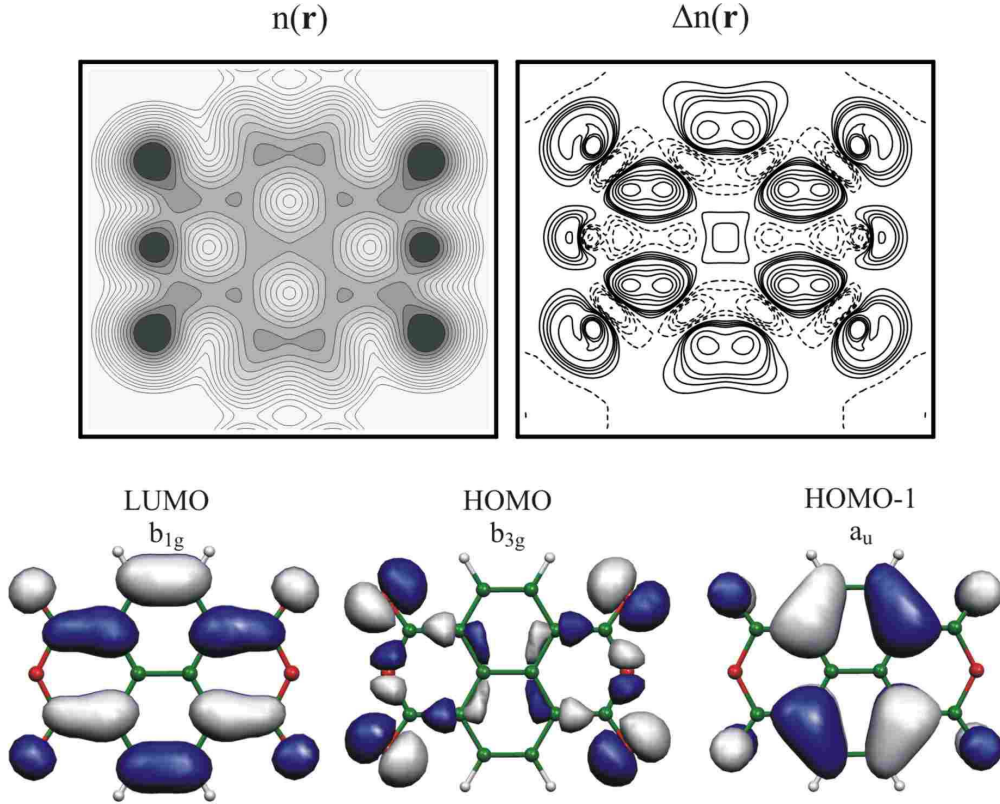


FIG. 3: (Color online) Top: Contours of the total electron density (left) and of the electron density difference (right) in a plane 0.5 Å below the NTCDA molecule at the top site; for Δn solid lines represent electron charge accumulation regions, broken lines - depletion regions. Bottom: 3D views of the LUMO (b_{1g} symmetry), HOMO (b_{3g}), and HOMO-1 (a_u) orbitals of the isolated NTCDA molecule. The distribution of accumulated charge closely resembles that of the LUMO of isolated NTCDA.

deduced⁹. Thus, our value of 0.92eV is reasonable, but is most probably an underestimate, keeping in mind that usually GGA functionals tend to underbind adsorbates on noble metals and that the adsorption energy on the Ag(110) face should be even larger than those two values. It is expected, however, that the *differences* between adsorption energies in different adsorption configurations should be more accurate.

These differences are quite significant. The top site is predicted to be by far the most stable one. Fink *et al.*⁸ in fact also proposed that the top site, with all oxygens sitting almost on top of silver atoms underneath, should be the most favorable adsorption configuration (see Fig. 6 in Ref. 8). The proposal was motivated by analogy with the local adsorption geometry of PTCDA on Ag(110), which had been determined in an elegant STM experiment³⁷, and noting that both PTCDA and NTCDA fit the Ag(110) template (PTCDA spans four, and NTCDA spans three atomic rows - see Fig. 1, T site, and Fig. 4 in Ref. 37). Our DFT calculations fully confirm this hypothesis. For NTCDA on Ag(110) the most favorable adsorption geometry is that for which oxygens lie directly above silver atoms in the $[1\bar{1}0]$ rows, just like

for PTCDA on Ag(110). For the latter system an earlier computational study based on the empirical Universal Force Field (UFF)³⁸, predicted instead an equilibrium configuration equivalent to LB. The second most stable configuration, SB (Fig. 1), is also characterized by oxygen atoms on top of atomic rows but shifted half a lattice constant in the $[1\bar{1}0]$ direction. Although this remains to be explored in detail, configuration SB is likely a transition state for diffusion along the Ag rows. In the case of the least favorable sites, LB and H, oxygen atoms sit between the close-packed rows. During the geometry optimization, carboxyl oxygens moved towards the substrate, causing a bending of the molecule, just like for PTCDA on Ag(111)¹⁵. In the relaxed geometries, carboxyl oxygens were approximately 0.25 Å and 0.30 Å closer to the silver substrate than the naphthalene core for the T and SB sites, respectively. For the T site, the carboxyl oxygens were situated 2.40 Å, the anhydride oxygens 2.50 Å, the carbons in the anhydride groups 2.54 Å, the carbons and hydrogens in the naphthalene core 2.62 Å from the topmost Ag(110) plane. An average distance of ~ 3.0 Å was obtained for NTCDA on the less reactive Ag(111) surface in a recent (NIXSW) experiment³⁹. On

Site	T	SB	H	LB
Adsorption energy E_{ad} [eV]	0.92	0.45	~ 0	~ 0
Charge ΔN [electrons]	0.38	0.37	0.34	0.35

TABLE I: Adsorption energies and net electron charges on the molecule determined from Eq. 2 after adsorption in four different sites.

one hand, the distance between the NTCDA molecule and the more reactive Ag(110) surface should indeed be smaller than on the close-packed Ag(111) surface. On the other hand, since the potential energy around the equilibrium molecule-metal distance is quite shallow in DFT, changes in that distance only lead to a tiny variation of the adsorption energy. Thus we conclude that the calculated distances are subject to larger errors than the adsorption energies themselves. During the geometry optimization, in the case of the favorable sites (T and SB), silver atoms just below the carboxyl oxygens moved upwards by 0.07 Å and 0.03 Å with respect to the average level of the top layer, thus further reducing the corresponding Ag-O distances. This naturally leads to the hypothesis that the interaction which leads to site-selectivity occurs between the carboxyl oxygens and the silver atoms in the [110] rows. If this is so, then what is the physical nature of this interaction?

To answer this question, we analyze the electron density redistribution caused by the adsorption of NTCDA at different sites by calculating the density difference

$$\Delta n = n^{\text{tot}} - n^{\text{sub}} - n^{\text{mol}}, \quad (1)$$

where n^{tot} is the total density of the system, and n^{sub} and n^{mol} are the densities of the substrate and molecule in their relaxed geometries. This function shows the charge rearrangement caused by adsorption of the molecule on the surface. Averages of the total densities and the density differences along the [110] and [001] directions, as well as xy -integrated densities and density differences, are shown in Fig. 2. From these plots and 3D representations of the density difference (not shown) one recognizes that (a) electron charge flows mainly from the metal to the molecule and (b) the charge accumulation region is closely related to the LUMO of the isolated molecule. This can clearly be seen in Fig. 3, where the total electron density along with density difference in a plane 0.5 Å below the molecule (in the T configuration) is compared to the LUMO (b_{1g} symmetry), HOMO (b_{3g}) and HOMO-1 (a_u) orbitals of the free NTCDA molecule⁴⁰. Practically no back-donation from occupied orbitals occurs. For NTCDA on Ag(111) NEXAFS studies of Gador *et al.*^{10,11} showed a partial filling of the π -type LUMO. Our results are consistent with this finding. Various approximate charge partitioning schemes exist which associate charge with particular subsystems of the total system. We define the net electron charge on the molecule as

$$\Delta N = \int_{z_0}^{z_1} \Delta n(z) dz, \quad (2)$$

where $\Delta n(z)$ is the xy -integrated density difference, z_0 is the coordinate for which $\Delta n(z_0)$ is zero (see Fig. 2), and z_1 lies in the middle of the vacuum region, where all densities are practically zero. The net electron charge, as well as the adsorption energies for all four sites are summarized in Table I. Thus NTCDA acquires about 0.3–0.4 electron charge upon adsorption. The charge transfer can be rationalized by the following simple argument. To a first approximation, the overall charge transfer is proportional to the difference of the chemical potentials of the substrate (referred to the vacuum level close to the surface of the metal) and of the molecule. The former is $\mu_{\text{sub}} = -\Phi_{\text{sub}}$, Φ_{sub} being the work function of the Ag(110) surface, namely 4.13 eV (computed value). The latter, the so-called charge neutrality level⁴¹, is approximately equal to the midgap position⁴²:

$$\mu_{\text{mol}} \approx \frac{e_{\text{HOMO}} + e_{\text{LUMO}}}{2} \approx -\frac{IP + EA}{2}, \quad (3)$$

where e_{HOMO} , e_{LUMO} are computed Kohn-Sham eigenvalues while IP and EA are the ionization potential and the electron affinity of the isolated molecule. According to the last expression on the right hand side, μ_{mol} is just the negative of the absolute electronegativity defined by Mulliken⁴³. In our case, $\mu_{\text{NTCDA}} \approx -5.9$ eV, which agrees very well with the experimental value -6.0 eV⁴⁴. Interestingly, the so-calculated absolute electronegativities are almost equal for NTCDA and PTCDA, even though the band gap is smaller for PTCDA than NTCDA. Thus, $\mu_{\text{sub}} > \mu_{\text{NTCDA}}$, so that electrons are transferred to the molecule, mainly to its LUMO. Such an interpretation is in agreement with chemical studies, since NTCDA is known to be an electron acceptor⁴⁵.

Charge transfer from the metal to the molecule leads to an increase of the work function of the combined system. From the total charge density distribution we obtain an increase $\Delta\Phi = +1.0$ eV. This corresponds to an induced negative electric dipole moment per NTCDA of 0.6 eÅ which is slightly smaller than the crude estimate $0.4e \times 2.5$ Å partially because the relaxation of the ion cores makes an opposite contribution to the net dipole. No measurements of the work function for NTCDA/Ag(110) are available at present. Hill *et al.*⁴⁶ found that the work function increases by $+0.2$ eV upon adsorption of a related molecule, 3,4,9,10-perylenetetracarboxylic bisimidazole on polycrystalline Ag. A similarly small value was found for NTCDA on Ag(111)^{19,47}. Since the Ag(111) surface has a higher work function, charge donation can be more substantial and $\Delta\Phi$ larger on the Ag(110) surface. However, our value of $+1.0$ eV is probably overestimated for two reasons. First, the calculated work function of the Ag(110) surface is slightly lower than the experimental one, and this favors charge donation to the LUMO of NTCDA. Second, as is well known, the band gaps of semiconductors⁴⁸ and of organic molecules⁴⁹ are underestimated in both LDA and GGA. The Kohn-Sham LUMO eigenvalue is usually lower in energy than the corresponding electron affinity level and this also leads to a

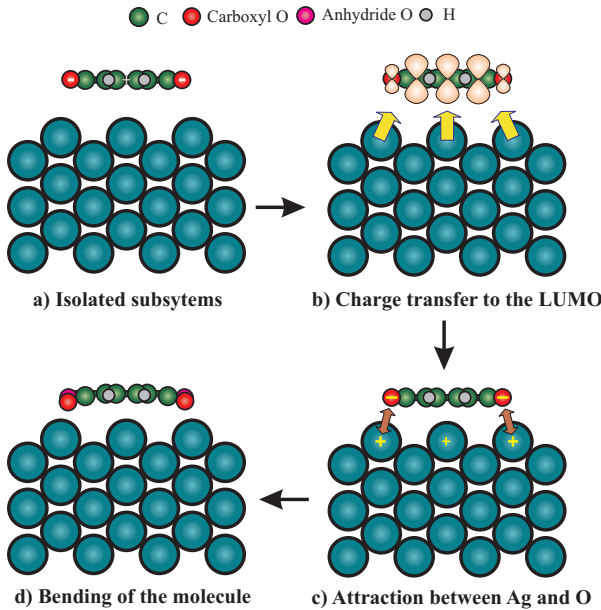


FIG. 4: (Color online) Sketch of the mechanism of adsorption of NTCDA on Ag(110), viewed along the $[1\bar{1}0]$ direction. (a) The two isolated subsystems: note the electron excess on the peripheral oxygens and the positive charge on the naphthalene core. (b) Charge transfer from the substrate to the molecule, mainly to its LUMO. (c) This transfer causes positive charging of the topmost silver layer and a local electrostatic attraction between silver atoms in the $[1\bar{1}0]$ rows below the negatively charged carboxyl oxygens. (d) The Ag-O attraction causes a distortion of NTCDA from planarity, with peripheral oxygens moving closer to the Ag rows than the naphthalene core.

stronger charge donation to the LUMO and thus to a larger $\Delta\Phi$. To cure these problems, expensive calculations at the level of self-consistent many-body perturbation theory, e.g. the GW-approximation⁵⁰, must be performed. We believe, however, that the above-mentioned issues will not affect the proposed model for the site-selective adsorption of NTCDA on the Ag(110) surface.

Table I shows that the overall charge on the molecule is very similar for all the adsorption sites studied and does not reflect the significant differences in adsorption energies. However, one notices from Fig. 2 that in the case of the favorable T and SB sites the charge transfer is stronger and more localized between the carboxyl oxygens and silver atoms underneath. Furthermore, the electrostatic energy gain crudely estimated by treating the molecule-metal system as a plane-parallel capacitor amounts to only 0.12 eV, i.e. much less than the actual electrostatic contribution to the adsorption energy in those favorable sites. This also speaks for the fact that site selectivity is determined by the proximity of carboxyl oxygens and silver atoms.

Our results suggest the following adsorption scenario of NTCDA on Ag(110) surface which leads to site-specific

bonding. As a result of charge transfer to the LUMO of the molecule, silver atoms in the topmost layer become slightly positively charged. Carboxyl oxygens, being negatively charged even in the free molecule (~ 0.2 electron excess), are then attracted by electrostatic forces to the substrate. This attraction is maximal when the Ag-O distance is minimal, that is in the T and SB configurations. Thus, changes in the electron density are bigger and more localized for these two sites (Fig. 2), as compared to the unfavorable LB and H configurations. The local Ag-O attraction leads to a distortion of NTCDA from planarity, i.e., the carboxyl oxygens move closer to the substrate than the naphthalene core. Most of these effects, together with changes in bond lengths which reflect the density distribution of the LUMO, have been found and discussed for PTCDA on Ag(111)¹⁵. It is interesting to note the qualitative similarity between those two systems despite the fact that both molecules and substrates are different. Bonds through which the nodal planes of the LUMO pass are slightly elongated (maximum 0.03 Å for the C=O bond), and the others are slightly contracted. However, as mentioned in the introduction, the bonding is stronger and more site specific for the more open Ag(110) surface. Furthermore, free electron-like surface states of the Ag(111) surface might also play a role in adsorption on that substrate. Figure 4 summarizes the mechanism of the bonding and bending of the molecule on the Ag(110) surface.

Concerning the lateral ordering of the molecules, we studied adsorption in the favored T configuration for two different lateral surface unit cells: (3,0/0,3) and the experimentally found (3,0/1,3)⁸. Both unit cells contain one molecule and the same number of substrate atoms and both structures are rather open. We found that the adsorption energies in both of these arrangements are essentially the same. This happens, most probably, because semilocal GGA functionals fail to describe long-range van-der-Waals interactions²², which are likely to be most important for the preference of one superstructure over the other.

IV. CONCLUSIONS

In conclusion, we have studied site-selective adsorption properties of NTCDA on the Ag(110) surface by means of density functional calculations. The interaction of the molecule with the substrate can be summarized by the following scenario: (1) NTCDA, being an electron acceptor, takes ~ 0.4 electron from the silver substrate and the LUMO is partially filled; (2) this transfer leads to a slight positive charging of the silver atoms in the topmost layer and weakening of the C=O bonds, thus enhancing the local electrostatic interaction between Ag atoms in the Ag $[1\bar{1}0]$ rows and carboxyl oxygens (this is the main difference between favorable and unfavorable sites); (3) the Ag-O attraction distorts the molecule from the planar configuration. Being quite similar to the mecha-

nism recently established for PTCDA on Ag(111)¹⁵, we believe that the proposed scenario is also applicable to the adsorption of PTCDA on Ag(110)³⁷. Experimentally found differences between different substrates^{16,17,18} are still to be explored in detail. Very recently, a single polar N-Cu bond was found to be responsible for bonding of inclined adenine on Cu(110)⁵¹, like for alkane-thiols on Au(111)²⁷, suggesting that local electrostatic bonding can occur for many organic molecules on open fcc(110) surfaces. In the case of aromatic acceptor molecules with several peripheral electronegative atoms (O, N, halogens) adsorbed flat on noble metal fcc(110) surfaces, the origin of site-selectivity is less obvious. Our results suggest that observed commensurate superstructures can arise from the close match of those atoms and electron-depleted

substrate atoms. DFT computations appear capable of grasping lateral variations of the resulting electrostatic interactions.

V. ACKNOWLEDGMENTS

We acknowledge the Computer Center of University of Basel for computational resources. We would like to thank S. Goedecker, L. Ramoino, and M. Rayson for discussions and comments on the manuscript. This work was financially supported by the Swiss NSF and the NCCR “Nanoscale Science”.

* Present address: *Institute of Theoretical Physics, École Polytechnique Fédérale de Lausanne (EPFL), CH-1015 Lausanne, Switzerland*

- ¹ S.R. Forrest, Chem. Rev. **97**, 1793 (1997); J. Phys. Cond. Mat **15**, S2599 (2003); Nature **428**, 911 (2004).
- ² S.M. Barlow and R. Raval, Surf. Sci. Rep. **50**, 201 (2003).
- ³ E. Umbach, K. Glöckler, and M. Sokolowski, Surf. Sci. **402**, 20 (1998).
- ⁴ H. Ishii, K. Sugiyama, E. Ito, and K. Seki, Adv. Mat. **11**, 605 (1999).
- ⁵ X.-U. Zhu, Surf. Sci. Rep. **56**, (2004); D.M. Adams *et al.*, J. Phys. Chem. B, **107**, 6668 (2003).
- ⁶ D. Cahen, A. Kahn, and E. Umbach, Materials Today July/August, 32 (2005).
- ⁷ F. Rosei, M. Schunack, Y. Naitoh, P. Jiang, A. Gourdon, E. Laegsgaard, I. Stensgaard, C. Joachim, and F. Besenbacher, Prog. Surf. Sci. **71**, 95 (2003).
- ⁸ R. Fink, D. Gador, U. Stahl, Y. Zou, and E. Umbach, Phys. Rev. B **60**, 2818 (1999).
- ⁹ U. Stahl, D. Gador, A. Soukopp, R. Fink, and E. Umbach, Surf. Sci. **414**, 423 (1998).
- ¹⁰ D. Gador, C. Buchberger, R. Fink, and E. Umbach, J. Electron Spectrosc. **96**, 11 (1998); *ibid.* **101-103**, 523 (1999).
- ¹¹ D. Gador, C. Buchberger, R. Fink, and E. Umbach, Europhys. Lett. **41**, 231 (1998).
- ¹² J. Taborski, P. Väterlein, H. Dietz, U. Zimmermann, and E. Umbach, J. of Electron Spectr. **75**, 129 (1995).
- ¹³ M. Eremtchenko, J.A. Schaefer, and F.S. Tautz, Nature **425**, 602 (2003).
- ¹⁴ M. Eremtchenko, D. Bauer, J.A. Schaefer, and F.S. Tautz, New J. Phys. **6**, 4 (2004).
- ¹⁵ A. Hauschild, K. Karki, B.C.C. Cowie, M. Rohlfing, F.S. Tautz, and M. Sokolowski, Phys. Rev. Lett. **94**, 036106 (2005).
- ¹⁶ F.S. Tautz, M. Eremtchenko, J.A. Schaefer, M. Sokolowski, V. Shklover, K. Glöckler, and E. Umbach, Surf. Sci. **502-503**, 176 (2002).
- ¹⁷ F.S. Tautz, S. Sloboshanin, J.A. Schaefer, R. Scholz, V. Shklover, M. Sokolowski, and E. Umbach, Phys. Rev. B **61**, 16933 (2001).
- ¹⁸ F.S. Tautz, M. Eremtchenko, J.A. Schaefer, M. Sokolowski, V. Shklover, and E. Umbach, Phys. Rev. B **65**, 125405 (2002).
- ¹⁹ A. Schöll, Y. Zou, Th. Schmidt, R. Fink, and E. Umbach, J. Phys. Chem. B **108**, 14741 (2004).
- ²⁰ R.M. Martin, *Electronic Structure. Theory and Practical methods* (Cambridge University Press, 2004).
- ²¹ M. Scheffler and C. Stampfl, in *Electronic Structure*, Vol. 2 of *Handbook of Surface Science*, edited by K. Horn and M. Scheffler (Elsevier, Amsterdam, 1999).
- ²² M. Dion, H. Rydberg, E. Schröder, D.C. Langreth, and B.I. Lundqvist, Phys. Rev. Lett. **92**, 246401 (2004).
- ²³ J.P. Perdew and S. Kurth, Springer Lecture Notes in Physics **620**, 1 (2003).
- ²⁴ W. Koch and M.C. Holthausen, *A Chemist’s Guide to Density Functional Theory* (Wiley-VCH, Weinheim, 2001).
- ²⁵ D. Lamoen, P. Ballone, and M. Parrinello, Phys. Rev. B **54**, 5097 (1996).
- ²⁶ L.-L. Wang and H.-P. Cheng, Phys. Rev. B **69**, 165417 (2004).
- ²⁷ H. Grönbeck, A. Curioni, and W. Andreoni, J. Am. Chem. Soc. **122**, 3839 (2000).
- ²⁸ L. Delle Site, C.F. Abrams, A. Alavi, and K. Kremer, Phys. Rev. Lett. **89**, 156103 (2002).
- ²⁹ Y. Morikawa, H. Ishii, and K. Seki, Phys. Rev. B **69**, 041403 (2004).
- ³⁰ S. Picozzi, A. Pecchia, M. Gheorghe, A. Di Carlo, P. Lugli, B. Delley, and M. Elstner, Phys. Rev. B **68**, 195309 (2003); Surf. Sci. **566**, 628 (2004).
- ³¹ L. Kröger, H. Jensen, R. Berndt, R. Rinaldi, and N. Lorente, cond-mat/0506025.
- ³² X. Gonze, J.-M. Beuken, R. Caracas, F. Detraux, M. Fuchs, G.-M. Rignanese, L. Sindic, M. Verstraete, G. Zerah, F. Jollet, M. Torrent, A. Roy, M. Mikami, Ph. Ghosez, J.-Y. Raty, and D.C. Allan, Comp. Mat. Sci. **25**, 478 (2002).
- ³³ J.P. Perdew, K. Burke, and M. Ernzerhof, Phys. Rev. Lett. **77**, 3865 (1996).
- ³⁴ S. Goedecker, M. Teter, and J. Hutter, Phys. Rev. B **54**, 1703 (1996).
- ³⁵ N. Troullier and J. L. Martins, Phys. Rev. B **43**, 1993 (1991).
- ³⁶ H.J. Monkhorst and J.D. Pack, Phys. Rev. B **13**, 5188 (1976).
- ³⁷ M. Böhringer, W.-D. Schneider, K. Glöckler, E. Umbach, and R. Berndt, Surf. Sci. **419**, L95 (1998); Phys. Rev. B

⁵⁷, 4081 (1998).
³⁸ C. Seidel, C. Awater, X.D. Liu, R. Ellerbrake, and H. Fuchs, *Surf. Sci.* **371**, 123 (1997).
³⁹ J. Stanzel, W. Weigand, L. Kilian, H.L. Meyerheim, C. Kumpf, and E. Umbach, *Surf. Sci.* **571** L311 (2004).
⁴⁰ The HOMO and HOMO-1 orbitals are almost energy-degenerate in PBE; other density functionals (BLYP, B3LYP, LDA) order them in slightly different ways.
⁴¹ H. Vazquez, R. Oswaldowski, P. Pou, J. Ortega, R. Perez, F. Flores, and A. Kahn, *Europhys. Lett.* **65**, 802 (2004); *Appl. Surf. Sci.* **234**, 107 (2004).
⁴² X. Crispin, V. Geskin, A. Crispin, J. Cornil, R. Lazzaroni, W.R. Salaneck, and J.-L. Bredas, *J. Am. Chem. Soc.* **124**, 9161 (2002).
⁴³ R.S. Mulliken, *J. Chem. Phys.* **2**, 782 (1934).
⁴⁴ A. Kahn, N. Koch, and W. Gao, *J. Polym. Sci. Polym. Phys.* **41**, 2529 (2003).
⁴⁵ R. Foster, *Organic Charge-Transfer Complexes* (Academic Press, New York, 1969).
⁴⁶ I.G. Hill, J. Schwartz, and A. Kahn, *Org. Elec.* **1**, 5 (2003).
⁴⁷ A. Schöll, L. Kilian, Y. Zou, T. Schmidt, R. Fink, and E. Umbach, (unpublished).
⁴⁸ R.O. Jones and O. Gunnarsson, *Rev. Mod. Phys.* **61**, 689 (1989).
⁴⁹ U. Salzner, J.B. Lagowski, P.G. Pickup, and R.A. Poirier, *J. Comp. Chem.* **18**, 1943 (1997).
⁵⁰ L. Hedin, *Phys. Rev.* **139**, A796 (1965).
⁵¹ M. Preuss, W. G. Schmidt, and F. Bechstedt, *Phys. Rev. Lett.* **94**, 236102 (2005).